Archives of Environmental Protection
Vol. 45 no. 4 pp. 92–103

PL ISSN 2083-4772
DOI 10.24425/aep.2019.130245

Adsorption of lead ions onto chemically activated carbon from waste tire char and optimization of the process using response surface methodology

Hilary Rutto*, Tumisang Seidigeng, Lucky Malise

Department of Chemical Engineering
Vaal University of Technology, South Africa

*Corresponding author's e-mail: hilaryr@vut.ac.za

Keywords: waste tire pyrolysis char, chemical activation, Central Composite Design (CCD), adsorption capacity, numerical optimization.

Abstract: Tires play an important role in the automobile industry. However, their disposal when worn out has adverse effects on the environment. The main aim of this study was to prepare activated carbon from waste tire pyrolysis char by impregnating KOH onto pyrolytic char. Adsorption studies on lead onto chemically activated carbon were carried out using response surface methodology. The effect of process parameters such as temperature (°C), adsorbent dosage (g/100 ml), pH, contact time (minutes) and initial lead concentration (mg/l) on the adsorption capacity were investigated. It was found out that the adsorption capacity increased with an increase in adsorbent dosage, contact time, pH, and decreased with an increase in lead concentration and temperature. Optimization of the process variables was done using a numerical optimization method. Fourier Transform Infrared Spectra (FTIR) analysis, X-ray Diffraction (XRD), Thermogravimetric analysis (TGA) and scanning electron microscope were used to characterize the pyrolytic carbon char before and after activation. The numerical optimization analysis results showed that the maximum adsorption capacity of 93.176 mg/g was obtained at adsorbent dosage of 0.97 g/100 ml, pH 7, contact time of 115.27 min, initial metal concentration of 100 mg/and temperature of 25°C. FTIR and TGA analysis showed the presence of oxygen containing functional groups on the surface of the activated carbon produced and that the weight loss during the activation step was negligible.

Introduction

With the continued increase in the use of auto mobiles, the generation of waste tires continues to increase rapidly every year throughout the world. The disposal of waste tyre poses a huge environmental concern. It has been reported that around 10 million waste tires are generated in South Africa every year and more than 5 million tons of waste tires are generated worldwide every year (Ariyadejwanich et al. 2003).

Previously, methods such as land filling, stock-pilling, and open dumping have been used for the disposal of waste tires, however, some drawbacks have been reported regarding such methods (Kotkowski et al. 2018). The disposal of waste tires through land fill sites causes environmental pollution since the waste tires are not biodegradable hence, they occupy huge spaces of the landfill sites (Mui et al. 2004). Stock-pilling and open dumping is said to be undesirable since waste tires pose fire hazards and can be a breeding ground for mosquitoes and vermin which can lead to health threats to humans (Betancur et al. 2009, Ko et al. 2004).

Recent research studies have focused on the utilization of waste tires through thermal processes such as direct combustion, gasification, pyrolysis for the disposal of waste tires, the recovery of valuable products and energy recovery (Molino et al. 2013, Murillo et al. 2006). These thermal treatment processes are also said to have the advantage of reducing the volume of the waste tires by 90% of its original volume after the thermal process (Sharma et al. 1998).

Out of all these thermal processes, pyrolysis of waste tires has received great attention and continues to do so due to its environmentally friendly nature compared to other thermal processes such as direct combustion (Sienkiewicz et al. 2012). In pyrolysis, the waste tires are subjected to thermal treatment inside a furnace at elevated temperatures under inert conditions. The products obtained from the pyrolysis of waste tires include pyrolytic oil, pyrolytic char, and pyrolysis gas which can all be upgraded into valuable products (Rudniak and Machniewski 2017). The char obtained from the pyrolysis of waste tires is said to have a high carbon content and thus can be used as carbon black or it can serve as a raw material to produce activated carbon (San Miguel et al. 2003). Activated carbon

from pyrolytic tire char can be obtained through an activation process. The activation process is necessary to ensure that the activated carbon produced contains improved adsorption characteristics for its application in adsorption processes.

There are two types of activation processes which can be applied in the preparation of activated carbon namely: physical activation and chemical activation (Ahmaruzzaman and Gupta 2011). Physical activation involves the use of oxidizing agents such as steam or CO_2 whereas chemical activation involves the impregnation of the carbon char with chemical agents such as potassium hydroxide (KOH), zinc chloride (ZnCl), phosphoric acid (H_3PO_4), nitric acid (HNO_3) and sodium hydroxide (NaOH) followed by carbonization to give a final product of activated carbon (Salehin et al. 2016).

Response Surface Methodology (RSM) is a collection of statistical and mathematical techniques used for the improvement, optimization and development of a process (Montgomery 2017). The main aim of RSM is to determine the optimum operating conditions for the process. From the method used to design experiments, RSM is used as a tool to improve the efficiency of the process by optimizing an output variable which is influenced by several independent variables (Amini et al. 2008, Tan et al. 2008). The input variables are varied during experimental test runs to evaluate how they affect the output variables and thus enable the possibility to identify the optimum operation conditions for the input variables (Garg et al. 2008).

In RSM, there are two types of design of experiments which are commonly used, namely central composite designs and Box Behnken designs (Rutto and Enweremadu 2012, Yusuf and Tekin 2017). Central composite design is commonly used to model a response variable with curvature by adding both center and axial points to a previously done factorial design (Ghaedi et al. 2015). In this study, central composite design was used to determine the effect of 5 process parameters on the adsorption capacity of waste tire derived activated carbon for the adsorption of lead ions from aqueous solution and to also optimize the adsorption capacity of the lead ions onto activated carbon. Optimization using RSM central composite design numerical optimization method is used in this study because RSM has the advantage of accounting for the interactive effects of the different variables which affect the response variable (Uzun and Şahan 2017).

In this study, activated carbon prepared from waste tire pyrolysis char was chemically impregnated with KOH to improve the adsorption characteristics of the activated carbon produced. The activated carbon produced was used as an adsorbent for the adsorption of lead ions from aqueous solution. Fourier Transform Infrared Spectra (FTIR) analysis, XRay Diffraction (XRD), Thermogravimetric analysis (TGA) and scanning electron microscope (SEM) were used to characterize the pyrolytic carbon char before and after activation.

Materials and methods

Adsorbent preparation

Waste tire pyrolysis char in a powder form was obtained from a local supplier. Firstly, 150 g of the char was washed with warm distilled water in order to remove impurities and then dried in a drying oven at 100°C overnight to remove moisture. After drying, the sample was sieved to a particle size less than 100 µm. 100 g of the sample was then impregnated with an aqueous mixture of KOH at an impregnation ratio (weight of KOH: weight of char) of 2:1 inside a 500 ml beaker and stirred for 24 hours at 80°C to aid the impregnation process. After mixing, the slurry mixture of the char and KOH was dried inside a drying oven for 24 hours. The dried chemically impregnated waste tire pyrolysis char was activated using a furnace under nitrogen atmosphere to ensure inert conditions for the activation process at 600°C for 60 minutes. After the activation the sample was washed with 1 M solution of HCl to remove the ash and sulphur content formed during the activation process. After washing with HCl the activated carbon was rinsed with distilled water until the pH of 7 and then dried inside a drying oven at 100°C for 24 hours.

Characterization of the adsorbent

Thermogravimetric analysis on pyrolysis char and activated carbon was performed using a Pyris 1 Perkin Elmer TGA instrument. The thermogravimetric analysis was done in the temperature range from 25 to 950°C at a heating rate of 10°C/minute.

Fourier Transform Infrared Radiation (FTIR) analysis was done to determine the functional groups present on the surface of the samples before activation and after the activation process. A Perkin Elmer spectrum (400 FT-IR/FT-NIR) was used and the samples were scanned and recorded in the range of 650–4000 cm^{-1} wave numbers under transmission mode detection.

A scanning Electron Microscope was used to study the morphology of the waste tire pyrolysis char and the waste tire activated carbon. The analysis was done using a Phillips XL 30S SEM. The process was done by scattering the samples on an adhesive carbon plate and sputter coating the sample with a thin layer of gold before the analysis with SEM.

XRD analysis was done on the waste tire pyrolysis char and the waste tire activated carbon to determine the phase analysis on the two samples. Sample preparation for the waste tire char and waste tire activated carbon was done using the black loading preparation method. A PANalytical Empyrean diffractometer with a PIXecl detector and fixed slits with Fe filtered Co-Kα radiation was used for the analysis. The phases were determined by using X'Pert High score plus software and the relative phase amounts (weight %) were estimated using the Reitveld method.

Batch adsorption procedure

Adsorption experiments were done using a shaking incubator operating at a constant shaking rate of 200 rpm. After adsorption process, the samples were quickly filtered using 125 µm filters and then the filtrates were diluted and analyzed for lead ions concentration using an atomic absorption spectrometer. The adsorption capacity of lead ions onto activated carbon adsorption was calculated using Equation 1.

$$q_e = \frac{(c_i - c_e)v}{w} \quad (1)$$

Where q_e is the equilibrium adsorption capacity of the activated carbon, C_i is the initial metal concentration before

the adsorption process (mg/l), C_e is the concentration of metal ions left in solution after equilibrium has been reached (mg/l), V is the volume of the solution used for the adsorption process (l), and W is the dry weight of the activated carbon used for the adsorption process in grams.

Central composite design experimental design for the optimization of parameters

For the adsorption of lead ions onto waste tire derived activated carbon, a response surface methodology used was central composite design for five independent variables (adsorbent dosage, initial metal concentration, pH, contact time, and temperature) with the response variable being the adsorption capacity of the lead ions onto waste tire activated carbon as shown in Table 1. The design consisted of α = 1 and five factors. The number of experiments which were obtained from the design was 50 batch adsorption experiments with 32 factorial points, 10 axial points, and 8 center points. Design expert 6.0.6 software was used. Eq. 2 was used to calculate the number of experiments required for the central composite design.

$$N = 2^n + 2n + nc \tag{2}$$

Where N is the number of experiments required for the design, n is the number of factors or independent variables, and nc is the replicate number of the center points in each experiment.

A mathematical model that relates the adsorption capacity to the process parameters through a third polynomial Equation 3 was used.

$$Y = \beta_O + \sum_{j=1}^{4} \beta_j X_j + \sum_{i,j=1}^{4} \beta_{ij} X_i X_j + \sum_{j=1}^{4} \beta_{jj} X_j^2 + \sum_{k,i,j=1}^{4} \beta_{kij} X_k X_i X_j + \sum_{j=1}^{4} \beta_{jjj} X_j^3 \tag{3}$$

Where Y is the predicted adsorption capacity (mg/g), β_o, β_j, β_{ij}, β_{jj}, β_{kij} and β_{jjj} represent the offset term, linear effect, first order interaction effect, squared effect, second order interaction effect and cubic effect respectively.

Model fitting and statistical analysis

The Design expert software 6.0.6 was used for regression analysis, the evaluation of the statistical significance and the fitting of model to a third order polynomial equation.

Results and discussions

Characterization of the adsorbent

Thermogravimetric analysis (TGA)

Thermogravimetric analysis was used to determine the thermal decomposition of waste tire pyrolytic char and the activated carbon derived from chemical activation.

Figure 1 shows the TGA and DTGA plots for the two samples, for both the raw char and chemically impregnated char. From Figure 1 it is visible that the weight loses are experienced in the temperature range of 50–900°C with regions of 50–100°C, 150–201°C, and again at 450–500°C appearing to be the most prominent regions where considerable weight loses were experienced. Similarly, previous studies have reported that the thermal decomposition of waste tires takes place in the temperature range of 200–500°C (Mui et al. 2010). The weight loss experienced at 50–100°C and 150–201°C can be attributed to the release of moisture from the samples. The weight loss experienced in the temperature range of 400–500°C can be attributed to the loss of volatile matter from the samples resulting from the incomplete pyrolysis of the waste tires.

At temperature above 500°C the weight loss experienced by the samples was low and took place at a lower rate. It can be clearly seen that there was a difference in weight loss in the two samples. There was more weight loss experienced in the chemically treated char and this is because the KOH used in the impregnation of the char acts as a dehydrating agent which enabled more volatile matter present in the char to be driven out and thus more pores were developed at the surface which can improve the adsorption process. Potassium hydroxide interacted with the carbon which catalyzes the dehydrogenation reaction producing a porous carbon. The mechanism at which the pores develop on the surface of activated char can be shown by the following redox reactions (Eq. 4–7) (Al-Rahbi and Williams 2016).

$$6KOH + 2C \rightarrow 2K + 2K_2CO_3 + 3H_2 \tag{4}$$

$$K_2CO_3 \rightarrow K_2O + CO_2 \tag{5}$$

$$K_2O + H_2 \rightarrow 2K + H_2O \tag{6}$$

$$6KOH + 2C \rightarrow 2K + 2K_2CO_3 + 3H_2 \tag{7}$$

During the activation, potassium hydroxide decomposed to potassium oxide as shown in Eq. 4 and the potassium oxide was reduced to potassium as shown in Eqs 5 and 6. The

Table 1. Experimental range and levels of variables chosen for this study

Variable	Coding	Units	Levels		
			-1	0	1
Adsorbent dosage	x_1	g/100ml	0.1	0.55	1
pH	x_2	–	2	4.5	7
Contact time	x_3	min	30	75	120
Initial metal concentration	x_4	mg/l	100	300	500
Temperature	x_5	°C	25	40	55

intercalation of potassium led to the opening of carbon pores hence making them porous.

Fourier Transform Infrared Spectra (FTIR)

The presence of oxygen containing functional groups on the surface of activated carbon has been reported to enhance the adsorption capacity of activated carbon for the adsorption of heavy metals (Park et al. 2016, Pradhan and Sandle 1999, Salehin et al. 2016). Figure 2 shows the FTIR spectra obtained for analyzing raw waste tire pyrolysis char and activated carbon produced by chemical activation with KOH. For the raw waste tire pyrolysis char, the functional groups present include the presence of bands at 960, 1550, 1816, 2112, 1996, 2354, 2677, 3419, and 3798 cm^{-1} wavenumbers. The band at 960 cm^{-1} can be attributed to the $= C - H$ bend in the alkenes group. The band at 1550 cm^{-1} can be attributed to the $N - O$ asymmetric stretch in the nitro compounds. The band experienced at 2112 cm^{-1} can be attributed to the $- C \equiv C -$ stretch in the alkynes group. For activated carbon derived from pyrolytic char, the bands experienced include those at 1000, 1348, 1740, 2110, and 2700 cm^{-1} wavenumbers. The band experienced at wavenumber 1000 cm^{-1} can be attributed to the strong $C - O$ stretch in the alcohols, carboxylic acids, esters, and ethers functional groups. The band experienced at 1348 cm^{-1} can be attributed to the $N - O$ symmetric stretch in the nitro compounds. The band experienced at 1740 cm^{-1} can be attributed to the strong $C = O$ stretch in the carbonyl and carboxylic acids groups. The band at 2110 cm^{-1} can be attributed to the $- C \equiv C -$ stretch in the alkynes group and lastly the band at 2700 cm^{-1} is attributed to the stretch of $H - C = O$ and $O - H$ in the aldehydes and carboxylic acids group respectively (Seng-eiad and Jitkarnka 2016). It has been reported that by chemically activating the waste tire char, prominent bands of oxygen containing functional groups were visible on the surface of the activated carbon produced which enhances the adsorption process (Aftab et al. 2016, Saleh and Gupta 2014).

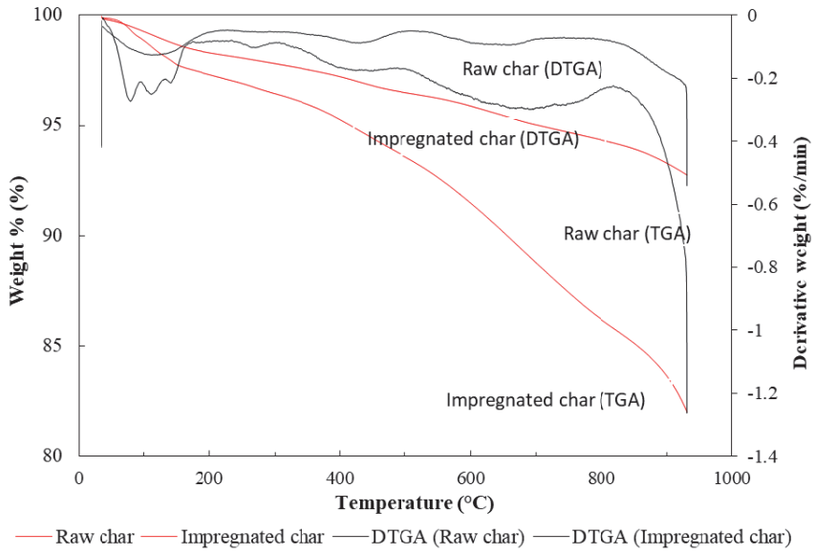

Fig. 1. TGA and DTGA plots for: (a) waste tire pyrolysis char and (b) chemically impregnated waste tire pyrolysis char

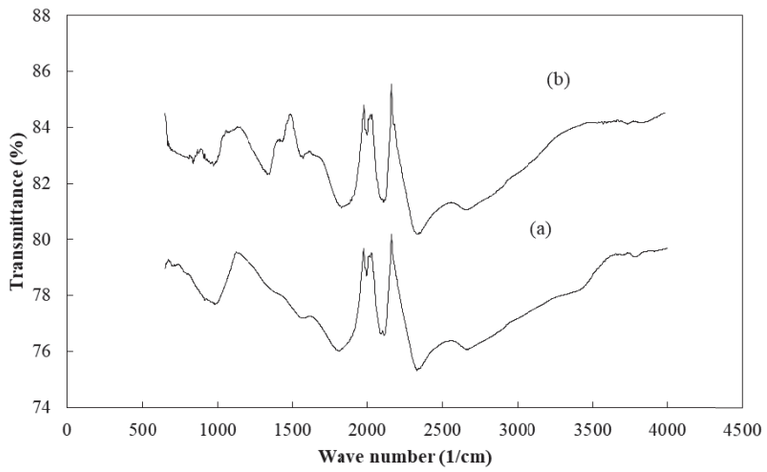

Fig. 2. Fourier Transform Infrared Spectra of (a) raw waste tire pyrolysis char and (b) chemically activated waste tire activated carbon

Scanning Electron Microscopy (SEM)

Scanning electron microscope (SEM) images depicted in Figure 3 displays the surface morphology of the waste tire pyrolysis char and waste tire activated carbon. The SEM image of the waste tire char shows that the morphology of the char consists of a surface which is dominated by large particles. On the other hand, the SEM image of the waste tire activated carbon shows that the morphology of the activated carbon consists of finer and porous particles on the surface of the waste tire activated carbon. This shows that chemical activation of the waste tire char produces waste tire activated carbon which has improved surface morphology.

X-Ray Diffraction (XRD) patterns

X-Ray Diffraction analysis was performed on the waste tire pyrolysis char and waste tire activated carbon as shown in Figure 4. Figure 4 shows the XRD patterns of the waste tire char and waste tire activated carbon. The XRD patterns show that the char had smaller diffraction peaks, which reveals its amorphous structure (Saravanan et al. 2013). The diffraction peaks of the waste tire activated carbon prepared at 600°C show that the waste tire activated carbon consists of sharp peaks at 2θ=36°, 55°, and 67°. The sharp peak experienced at 2θ=36° shows the presence of the wurtzite and sphalerite crystal phases (Saleh and Gupta 2012, Saravanan et al. 2015). This reveals the crystalline nature of the activated carbon produced.

Development of regression model equation

Table 2 shows the experimental design matrix and the results obtained for the adsorption of lead ions onto waste tire derived activated carbon. Table 2 shows the experimental design matrix results obtained for the response which was the adsorption capacity. Central composite design was the type of response surface methodology used to determine the relationship between the dependent process parameters, namely, adsorbent dosage, pH, contact time, initial metal concentration and temperature as well as independent variable, and the adsorption capacity. From Table 2 the adsorption capacity obtained when varying these process variables ranges from 3.2 to 94.1 mg/g depending on the process conditions. This shows that the process parameters have a significant effect on the adsorption capacity. Furthermore, the experimental results obtained were fitted with the second order polynomial equation is shown in Eq. 8.

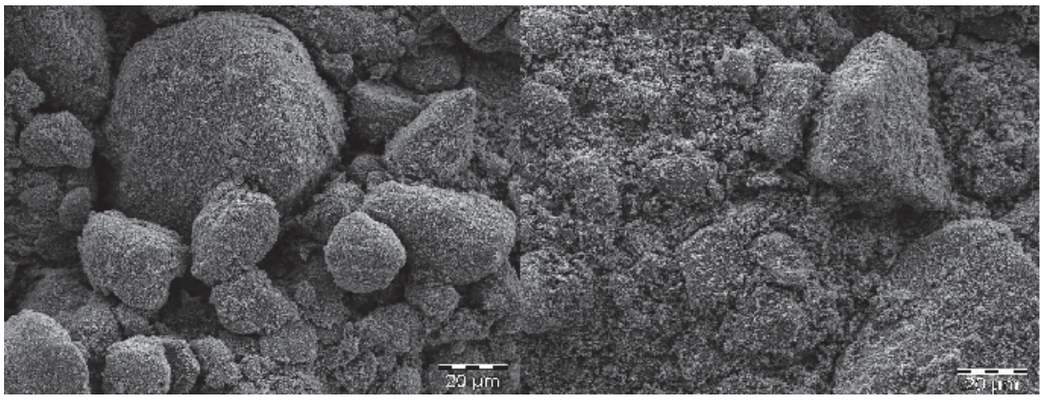

(a) (b)

Fig. 3. Scan electron micrographs of (a) waste tire pyrolysis char and (b) waste tire activated carbon

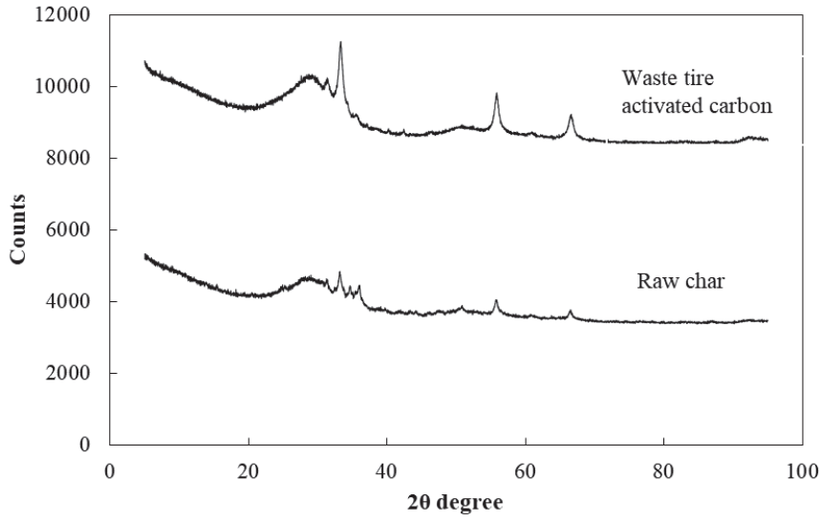

Fig. 4. XRD patterns for waste tire pyrolysis char and waste tire activated carbon

$$Y = 26.49138 + 3.835294x_1 + 7.220588x_2 + 4.255882x_3 - 23.8382x_4 - 3.44412x_5 - 1.53276x_1^2 - 1.88276x_3^2 + 11.11724x_4^2 + 1.317241x_5^2 + 2.96875x_1x_2 + 2.69375x_1x_3 - 0.76875x_1x_4 - 1.30625x_1x_5 + 0.3x_2x_3 - 2.85x_2x_4 - 3.3125x_2x_5 - 2.6125x_3x_4 - 0.9625x_3x_5 + 0.1x_4x_5 \quad (8)$$

The positive sign in front of the terms specifies a synergistic effect, while the negative sign indicates an antagonistic effect (Ghaedi et al. 2015). The coefficient correlation (R^2) can be used to evaluate the quality of the model. The R^2 for Eq. 8 is 0.9625. This suggests that 96.3% of the total deviation in the adsorption capacity responses is clarified by the model.

Figure 5 shows a plot of the experimental values against the predicted values of adsorption capacity plotted against a unit slope. The results indicate that the regression model was accurate in predicting the experimental data.

Model adequacy check

The analysis of variance (ANOVA) that was used to verify the acceptability of the model is shown in Table 3. The cubic model was verified at a 95% confidence level and was found to be significant since the computed value (37.23) was higher than theoretical $F_{0.05\ (20,\ 29)}$ (3.96). This shows that the regression model is accurate in predicting the adsorption capacity. As shown in Table 3 it was observed that generally the initial metal concentration (x_4) had the most noticeable effect due to the large value of its sum squares; it was followed by pH (x_2), contact time (x_3), adsorbent dosage (x_1) and temperature (x_5) in respective descending order. All the process variables had a significant effect on the adsorption capacity based on a 95% confidence level.

Table 2. Experimental design matrix and results for the adsorption of lead ions onto waste tire derived activated carbon

Run	Adsorbent dosage x_1 (g/100ml)	pH x_2	Experimental variables		Response variable	
			Contact time x_3 (min)	Initial metal concentration x_4 (mg/l)	Temperature x_5 (°C)	Adsorption capacity y (mg/g)
1	0.1	2	30	100	25	45.8
2	1	2	30	100	25	33
3	0.1	7	30	100	25	60.7
4	1	7	30	100	25	78
5	0.1	2	120	100	25	50.7
6	1	2	120	100	25	57.4
7	0.1	7	120	100	25	70.6
8	1	7	120	100	25	94.1
9	0.1	2	30	500	25	6.8
10	1	2	30	500	25	3.2
11	0.1	7	30	500	25	11.3
12	1	7	30	500	25	20.3
13	0.1	2	120	500	25	7.8
14	1	2	120	500	25	8.3
15	0.1	7	120	500	25	7.9
16	1	7	120	500	25	40.1
17	0.1	2	30	100	55	40.4
18	1	2	30	100	55	46.8
19	0.1	7	30	100	55	56.8
20	1	7	30	100	55	50.7
21	0.1	2	120	100	55	50.3
22	1	2	120	100	55	58.6
23	0.1	7	120	100	55	56.9
24	1	7	120	100	55	77.8
25	0.1	2	30	500	55	4.5
26	1	2	30	500	55	5
27	0.1	7	30	500	55	10.9

Run	Adsorbent dosage x_1 (g/100ml)	pH x_2	Experimental variables		Response variable	
			Contact time x_3 (min)	Initial metal concentration x_4 (mg/l)	Temperature x_5 (°C)	Adsorption capacity y (mg/g)
28	1	7	30	500	55	9
29	0.1	2	120	500	55	5.8
30	1	2	120	500	55	4.2
31	0.1	7	120	500	55	6.5
32	1	7	120	500	55	11
33	0.1	4.5	75	300	40	12.1
34	1	4.5	75	300	40	38.7
35	0.55	2	75	300	40	19.3
36	0.55	7	75	300	40	30.8
37	0.55	4.5	30	300	40	15.6
38	0.55	4.5	120	300	40	35.5
39	0.55	4.5	75	100	40	60.3
40	0.55	4.5	75	500	40	15.8
41	0.55	4.5	75	300	25	36.4
42	0.55	4.5	75	300	55	20.1
43	0.55	4.5	75	300	40	25.7
44	0.55	4.5	75	300	40	30.1
45	0.55	4.5	75	300	40	24.7
46	0.55	4.5	75	300	40	32.8
47	0.55	4.5	75	300	40	26.4
48	0.55	4.5	75	300	40	24.7
49	0.55	4.5	75	300	40	20
50	0.55	4.5	75	300	40	24

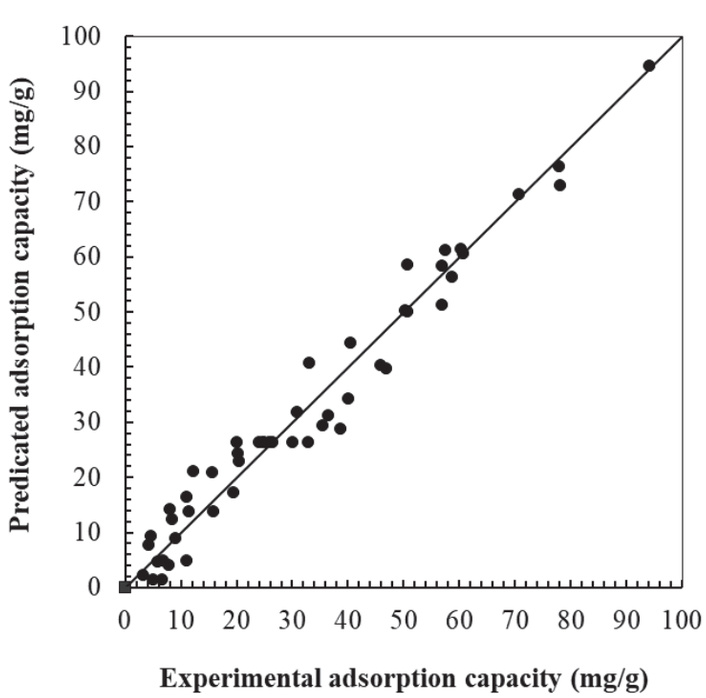

Fig. 5. Predicted versus the experimental values of the adsorption capacity

Table 3. Analysis of variance table for the adsorption capacity of waste tire derived activated carbon in the removal of lead ions from aqueous solution

Source	Sum of Squares	DF	Mean Square	F Value	Prob>F	
Model	24846.91	20	1242.346	37.23857	< 0.0001	significant
x_1	500.1224	1	500.1224	14.99087	0.0006	
x_2	1772.654	1	1772.654	53.13426	< 0.0001	
x_3	615.8262	1	615.8262	18.45902	0.0002	
x_4	19320.89	1	19320.89	579.1321	< 0.0001	
x_5	403.3062	1	403.3062	12.08886	0.0016	
x_1^2	5.810757	1	5.810757	0.174174	0.6795	
x_2^2	8.767473	1	8.767473	0.2628	0.6121	
x_3^2	4.729093	1	4.729093	0.141752	0.7093	
x_4^2	305.6886	1	305.6886	9.162832	0.0051	
x_5^2	4.291567	1	4.291567	0.128637	0.7224	
x_1x_2	282.0313	1	282.0313	8.453718	0.0069	
x_1x_3	232.2013	1	232.2013	6.960094	0.0133	
x_1x_4	18.91125	1	18.91125	0.566853	0.4576	
x_1x_5	54.60125	1	54.60125	1.63664	0.2109	
x_2x_3	2.88	1	2.88	0.086326	0.7710	
x_2x_4	259.92	1	259.92	7.790946	0.0092	
x_2x_5	351.125	1	351.125	10.52476	0.0030	
x_3x_4	218.405	1	218.405	6.546559	0.0160	
x_3x_5	29.645	1	29.645	0.888591	0.3536	
x_4x_5	0.32	1	0.32	0.009592	0.9227	
Residual	967.4922	29	33.3618			

The quadratic terms x_4, had more influence on the adsorption capacity based on 95% confidence level. Variables x_2, x_1, x_3, and x_5 had minor influence on the adsorption capacity in respective descending order. The cubic terms do not affect the adsorption capacity. The interaction amongst the variables (x_2x_5), (x_1x_2), (x_2x_4), (x_1x_3) and (x_3x_4) has a significant impact on the adsorption capacity in descending order. The interaction terms (x_1x_5), (x_3x_5), (x_1x_4), (x_2x_3) and (x_4x_5) were non-significant based on 95% confidence level.

Effect of adsorbent dosage and pH on the adsorption of lead on activated carbon derived from waste tire pyrolytic char

Figure 6 displays the variations in adsorption capacity with the changes in the adsorbent dosage (x_1) and pH (x_2). The contact time (x_3), initial metal concentration (x_4) and temperature (x_5) were kept constant at 75 minutes, 300 ppm and 40°C respectively.

As shown in Figure 6(a), when pH of the solution increases there is an increase in the adsorption capacity. This is because at low pH the lead ions compete with hydrogen ions for the adsorption sites on the surface of the activated carbon leading to low adsorption capacities. But however, as the pH value increases the hydrogen ions in the solution decreases and provide less competition for lead ions on the adsorption sites of the activated carbon and this leads to an increase in the adsorption capacity (Rao et al. 2016, Saleh et al. 2013). As shown in Figure 6(b), at high pH of 7 as the adsorption dosage is increased the adsorption capacity increases significantly. At low pH of 2 as the adsorbent dosage is increased there is a slight increase in the adsorption capacity and adsorption capacity decreases at higher adsorbent dosage.

Effect of pH and contact time on the adsorption of lead on activated carbon derived from waste tire pyrolytic char

Figure 7 depicts the variations in adsorption capacity with the changes in pH (x_2) and contact time (x_4). The adsorbent dosage (x_1), initial metal concentration (x_4) and temperature (x_5) were kept constant at 0.55g/100ml, 300 ppm and 40°C respectively.

Figure 7(a) shows the effect of pH and contact time on the adsorption capacity of the lead ions onto activated carbon. The adsorption capacity increases with an increase in contact time and pH. This is because lead ions can be in contact with the waste tire activated carbon for prolonged period which yields to higher adsorption capacities. Low adsorption capacities at low pH values have been reported to take place due to the presence of hydrogen ions in solution at low pH. As explained, the

hydrogen ions compete with lead ions for the adsorption sites on the surface of the activated carbon leading to low adsorption capacities for lead ions adsorption (Rao et al. 2016, Saleh et al. 2013). However, as the pH value of the solution was increased the competition of the adsorption active sites decreased and the adsorption capacity increased. Two-dimensional plots in Figure 7(b) show that as pH increases, the adsorbent capacity increases at high and low contact time.

Effect of contact time and initial metal concentration on the adsorption of lead onto activated carbon derived from waste tire pyrolytic char

Figure 8 depicts the variations in adsorption capacity with the changes in the contact time (x_3) and initial metal concentration (x_4). The adsorbent dosage (x_1), pH (x_2) and temperature (x_5) were kept constant at 0.55g/100ml, 4.5 and 40°C respectively.

As shown in Figure 8(a) there was a slight increase in the adsorption capacity as the contact time was increased. However, as the initial metal concentration increased there was a decrease in the amount of adsorption capacity. This can be explained as follows, at low initial metal concentration there is low competition for the adsorption sites on the surface of the activated carbon, and this means that more adsorption will be taking place hence a higher adsorption capacity is expected at low initial metal concentration. However, at high initial metal concentration there is more competition for the adsorption active site and eventually the adsorption site of the activated carbon derived from waste tire pyrolytic char becomes saturated and hence there will be a reduction in the adsorption capacity. This is in an excellent agreement with the results obtained by Rao et al. 2016. As shown in Figure 8(b) when the contact time increased, there was an increase and slight increase in the adsorption capacities at low and high metal initial concentration respectively.

Effect of initial metal concentration and temperature on the adsorption of lead onto activated carbon derived from waste tire pyrolytic char

Figure 9 depicts the variations in adsorption capacity with the changes in the initial metal concentration (x_4) and temperature (x_5). The adsorbent dosage (x_1), pH (x_2) and contact time (x_3) were kept constant at 0.55g/100ml, 4.5 and 75 minutes respectively.

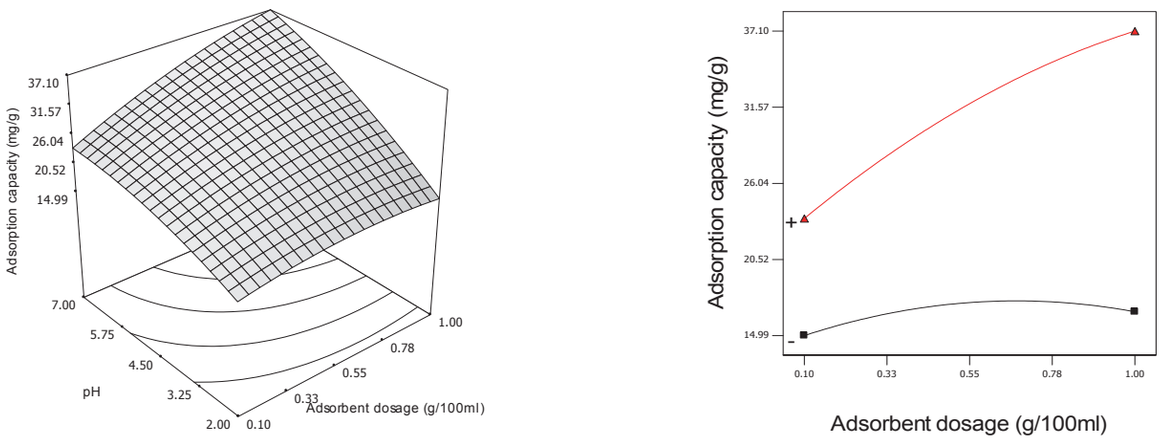

Fig. 6. The effect of pH and adsorbent dosage on the adsorption capacity of lead onto activated carbon derived from waste tyre char: (a) surface response plot and (b) two-dimensional plot where pH is held at + 7 and – 2

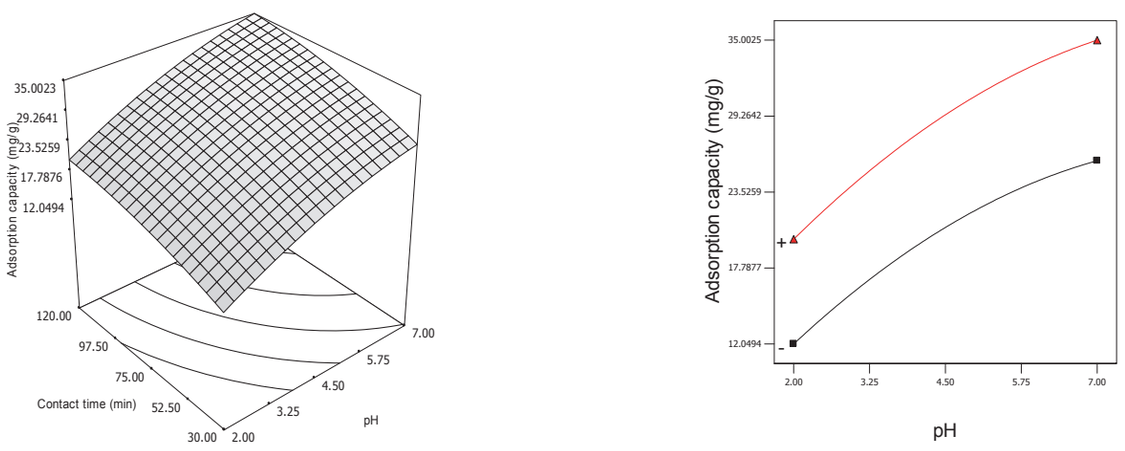

Fig. 7. The effect of pH and contact time on the adsorption capacity of lead onto activated carbon derived from waste tire pyrolytic char: (a) surface response plot and (b) two-dimensional plot where contact time is held at + 120 minutes and – 30 minutes

As shown in Figure 9(a), when the temperature increases there is a significant decrease in the adsorption capacity. A decrease in the adsorption capacity at a higher temperature suggests that the thermodynamic process is exothermic in nature (Saleh et al. 2014). Similar results were obtained by Rao et al. (2016) in their work on the adsorption of lead ions onto activated carbon derived from biomass. Another possible explanation for these results is that the adsorption sites on the surface of the activated carbon are more activate at lower temperatures than at elevated temperatures, where the adsorptive forces between the activated carbon and lead ions are weaker. The two-dimensional plot in Figure 9(b) shows that as the initial concentration was increased, there was a decrease in adsorption capacity at low and high temperatures.

Numerical process optimization

In RSM once the appropriate model has been established it is possible to optimize the response variable. In this study, the method of optimization applied was the numerical method. In numerical optimization, it is crucial to select the goal or objective function for each variable and the response (Amini et al. 2008). The goals for each variable are set as of maximum, minimum, in range, target, equal to or none for the response only. In Figure 10, the numerical optimization analysis results showed that the maximum adsorption capacity of 93.176 mg/g was obtained at adsorbent dosage, pH value, contact time, initial metal concentration and temperature of 0.97 g/100 ml, 7, 115.27 min, 100 mg/l and 25°C respectively. For this optimization, the desirability obtained is 0.994 which shows that the response does not fall outside of the desirable limits and this suggests that the optimized operating conditions can be relied on in achieving the optimum adsorption capacity provided by the model. Figure 10 shows an elaborate overview of the process optimization of all the parameters used. Table 4 shows a comparison of the different adsorbents used for the adsorption of lead ions using central composite design numerical optimization method.

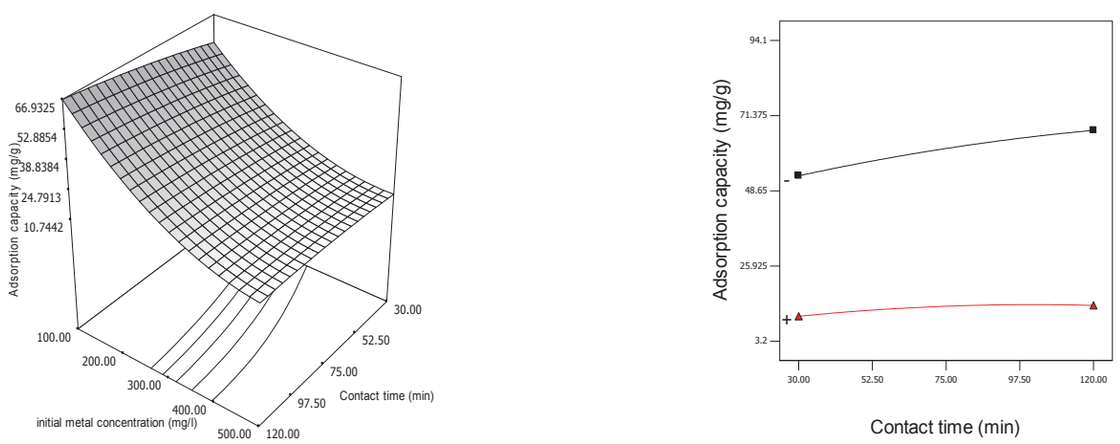

(a) (b)

Fig. 8. The effect of contact time and initial metal concentration on the adsorption capacity of lead onto activated carbon derived from waste tyre char: (a) surface response plot and (b) two-dimensional plot where initial metal concentration is held at + 500 ppm and – 100 ppm

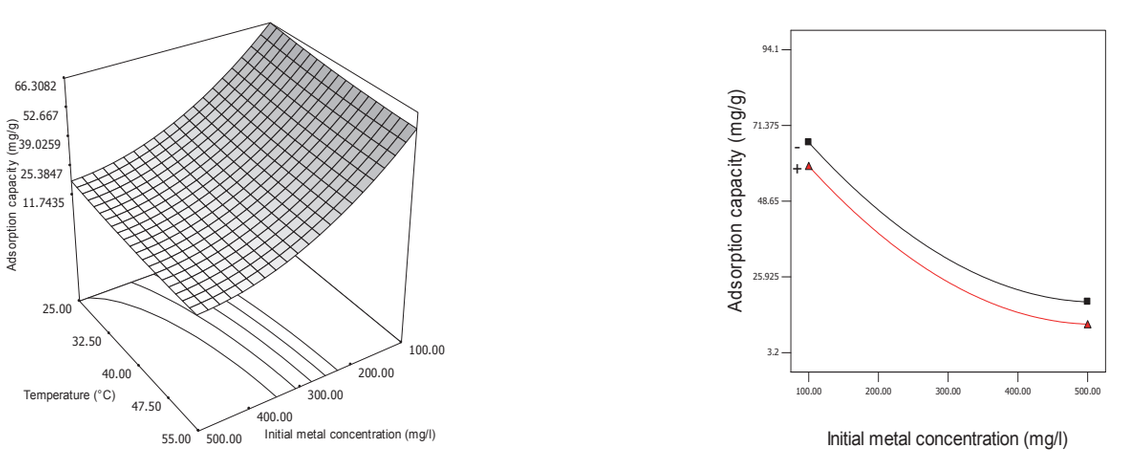

(a) (b)

Fig. 9. The effect of initial metal concentration and temperature on the adsorption capacity of lead onto activated carbon derived from waste tyre char: (a) surface response plot and (b) two-dimensional plot where the temperature is held at + 55°C and 25°C

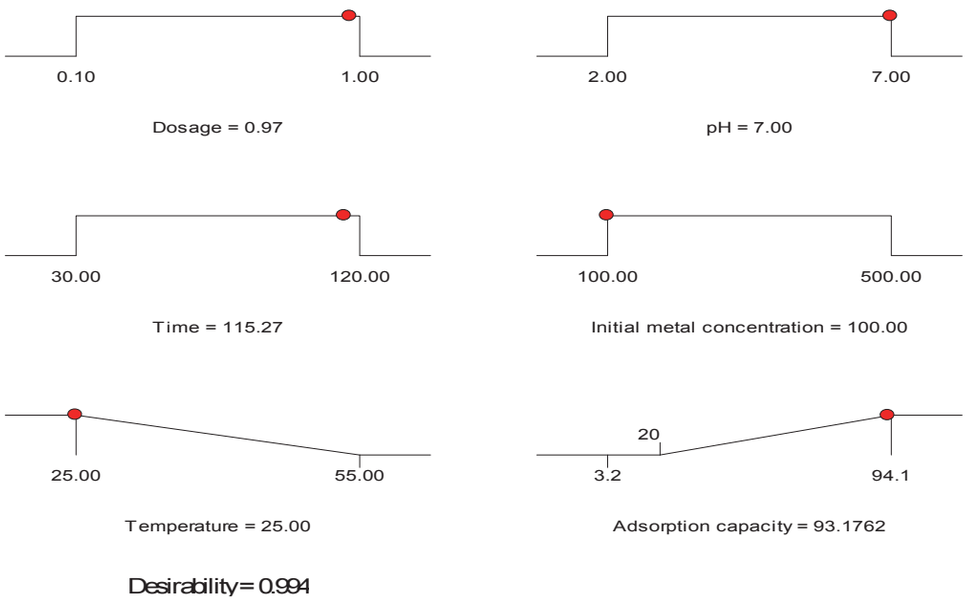

Fig. 10. Numerical optimization desirability ramps for the optimization of six goals (adsorbent dosage, pH, contact time, initial metal concentration, temperature, and adsorption capacity)

Table 4. Comparison of different adsorbents for the adsorption of lead ions using response surface methodology central composite design numerical optimization

Adsorbent used	Adsorption capacity achieved	Reference
Aspergillus niger	4.61 mg/g	Amini et al. 2008
Agricultural waste biomass	64 mg/g	Garg et al. 2008
Oryza sativa L. husk	8.60 mg/g	Zulkali et al. 2006
Waste tire activated carbon	93.176 mg/g	This study

Conclusion

The present study shows that it was possible to produce activated carbon from waste tire pyrolysis char using chemical activation with KOH. Characterization was done on the activated carbon produced and compared to that of waste tire pyrolysis char. The effect of process variables, namely, adsorbent dosage, pH, contact time, initial metal concentration, and temperature on the adsorption capacity of the activated carbon onto lead ions was done using RSM central composite design. Optimization was done using numerical analysis. FTIR and TGA analysis proved that activating the waste tire pyrolysis char with KOH showed the presence of oxygen containing functional groups on the surface of the activated carbon and that the activation process leads to the formation of pores on the activated carbon. A polynomial mathematical model was developed to correlate the process variables to the adsorption capacity. The adsorption capacity increased with an increase in adsorbent dosage, contact time, and pH, and decreased with an increase in lead concentration and temperature. The numerical optimization analysis results showed that the maximum adsorption capacity of 93.176 mg/g was obtained at adsorbent dosage, pH value, contact time, initial metal concentration and temperature of 0.97 g/100 ml, 7, 115.27 min, 100 mg/l and 25°C respectively. For this optimization, the desirability obtained is 0.994.

References

Aftab, T., Bashir, F., Khan, R.A. & Iqbal, J. (2016). Treatment of color through the adsorption efficiency of waste tire--derived char using response surface methodology, *Desalination and Water Treatment*, 57, 22, pp. 10324–10332, DOI: 10.1080/19443994.2015.1040460.

Ahmaruzzaman, M. & Gupta, V.K. (2011). Rice husk and its ash as low-cost adsorbents in water and wastewater treatment, *Industrial & Engineering Chemistry Research*, 50, 24, pp. 13589–13613, DOI: 10.1021/ie201477c.

Al-Rahbi, A.S. & Williams, P.T. (2016). Production of activated carbons from waste tyres for low temperature NOx control, *Waste Management*, 49, pp. 188–195, DOI: 10.1016/j.wasman.2016.01.030.

Amini, M., Younesi, H., Bahramifar, N., Lorestani, A.A.Z., Ghorbani, F., Daneshi, A. & Sharifzadeh, M. (2008). Application of response surface methodology for optimization of lead biosorption in an aqueou solution by Aspergillus niger, *Journal of Hazardous Materials*, 154, 1–3, pp. 694–702, DOI: 10.1016/j.jhazmat.2007.10.114.

Ariyadejwanich, P., Tanthapanichakoon, W., Nakagawa, K., Mukai, S. & Tamon, H. (2003). Preparation and characterization of mesoporous activated carbon from waste tires, *Carbon*, 41, 1, pp. 157–164, DOI: 10.1016/S0008-6223(02)00267-1.

Betancur, M., Martínez, J.D. & Murillo, R. (2009). Production of activated carbon by waste tire thermochemical degradation with

CO_2, *Journal of Hazardous Materials*, 168, 2–3, pp. 882–887, DOI: 10.1016/j.jhazmat.2009.02.167.

Garg, U.K., Kaur, M., Garg, V. & Sud, D. (2008). Removal of nickel (II) from aqueous solution by adsorption on agricultural waste biomass using a response surface methodological approach, *Bioresource Technology*, 99, 5, pp. 1325–1331, DOI: 10.1016/j.biortech.2007.02.011.

Ghaedi, M., Hajjati, S., Mahmudi, Z., Tyagi, I., Agarwal, S., Maity, A. & Gupta, V.K. (2015). Modelling of competitive ultrasonic assisted removal of the dyes – methylene blue and safranin-O using Fe_3O_4 nanoparticles, *Chemical Engineering Journal*, 268, pp. 28–37, DOI: 10.1016/j.cej.2014.12.090.

Ko, D.C., Mui, E.L., Lau, K.S. & McKay, G. (2004). Production of activated carbons from waste tire–process design and economic analysis, *Waste Management*, 24, 9, pp. 875–888, DOI: 10.1016/j.wasman.2004.03.006.

Kotkowski, T., Cherbanski, R. & Molga, E. (2018). Acetone adsorption on CO2-activated tyre pyrolysis char – thermogravimetric analysis, *Chemical & Process Engineering*, 39, 2, pp. 233–246, DOI: 10.24425/122946.

Molino, A., Erto, A., Natale, F.D., Donatelli, A., Iovane, P. & Musmarra, D. (2013). Gasification of granulated scrap tires for the production of syngas and a low-cost adsorbent for Cd(II) removal from wastewaters, *Industrial & Engineering Chemistry Research*, 52, 34, pp. 12154–12160, DOI: 10.1021/ie4012084.

Montgomery, D.C. (2001). *Design and analysis of experiments*, John Wiley and Sons Ltd, New York 2001.

Mui, E.L., Ko, D.C. & McKay, G. (2004). Production of active carbons from waste tyres – a review, *Carbon*, 42, 14, pp. 2789–2805, DOI: 10.1016/j.carbon.2004.06.023.

Mui, E.L.K., Cheung, W.H., Valix, M. & McKay, G. (2010). Mesoporous activated carbon from waste tyre rubber for dye removal from effluents, *Microporous and Mesoporous Materials*, 130, 1–3, pp. 287–294, DOI: 10.1016/j.micromeso.2009.11.022.

Murillo, R., Aylón, E., Navarro, M., Callén, M., Aranda, A. & Mastral, A. (2006). The application of thermal processes to valorise waste tyre, *Fuel Processing Technology*, 87, 2, pp. 143–147, DOI: 10.1016/j.fuproc.2005.07.005.

Park, J., Ok, Y.S., Kim, S., Cho, J., Heo, J., Delaune, R.D. & Seo, D. (2016). Competitive adsorption of heavy metals onto sesame straw biochar in aqueous solutions, *Chemosphere*, 142, pp. 77–83, DOI: 10.1016/j.chemosphere.2015.05.093.

Pradhan, B.K. & Sandle, N. (1999). Effect of different oxidizing agent treatments on the surface properties of activated carbons, *Carbon*, 37, 8, pp. 1323–1332, DOI: 10.1016/S0008-6223(98)00328-5.

Rao, H.J., King, P. & Kumar, Y.P. (2016). Experimental investigation on adsorption of lead from aqueous solution using activated carbon from the waste rubber tire: optimization of process parameters using central composite design, *Rasayan Journal of Chemistry*, 9, 2, pp. 254–277.

Rudniak, L. & Machniewski, P.M. (2017). Modelling and experimental investigation of waste tyre pyrolysis process in a laboratory reactor, *Chemical and Process Engineering*, 38, 3, pp. 445–454, DOI: 10.1515/cpe-2017-0034.

Rutto, H. & Enweremadu, C. (2012). Dissolution of a South African calcium based material using urea: an optimized process, *Korean Journal of Chemical Engineering*, 9, pp. 1–8, DOI: 10.1007/s11814-011-0136-z.

Saleh, T.A. & Gupta, V.K. (2012). Photo-catalyzed degradation of hazardous dye methyl orange by use of a composite catalyst consisting of multi-walled carbon nanotubes and titanium dioxide, *Journal of Colloid and Interface Science*, 371, 1, pp. 101–106, DOI: 10.1016/j.jcis.2011.12.038.

Saleh, T.A., Al-Saadi, A.A. & Gupta, V.K. (2014). Carbonaceous adsorbent prepared from waste tires: experimental and computational evaluations of organic dye methyl orange, *Journal of Molecular Liquids*, 191, pp. 85–91, DOI: 10.1016/j.molliq.2013.11.028.

Saleh, T.A., Gupta, V.K. & Al-Saadi, A.A. (2013). Adsorption of lead ions from aqueous solution using porous carbon derived from rubber tires: experimental and computational study, *Journal of Colloid and Interface Science*, 396, pp. 264–269, DOI: 10.1016/j.jcis.2013.01.037.

Saleh, T.A. & Gupta, V.K. (2014). Processing methods, characteristics and adsorption behavior of tire derived carbons: a review, *Advances in Colloid and Interface Science*, 211, pp. 93–101, DOI: 10.1016/j.cis.2014.06.006.

Salehin, S., Aburizaiza, A.S. & Barakat, M. (2016). Activated carbon from residual oil fly ash for heavy metals removal from aqueous solution, *Desalination and Water Treatment*, 57, 1, pp. 278–287, DOI: 10.1080/19443994.2015.1006824.

San Miguel, G., Fowler, G.D. & Sollars, C.J. (2003). A study of the characteristics of activated carbons produced by steam and carbon dioxide activation of waste tyre rubber, *Carbon*, 41, 5, pp. 1009–1016, DOI: 10.1016/S0008-6223(02)00449-9.

Saravanan, R., Karthikeyan, S., Gupta, V.K., Sekaran, G., Narayanan, V. & Stephen, A. (2013). Enhanced photocatalytic activity of ZnO/CuO nanocomposite for the degradation of textile dye on visible light illumination, *Materials Science and Engineering*, 33, 1, pp. 91–98, DOI: 10.1016/j.msec.2012.08.011.

Saravanan, R., Mansoob, K.M., Gupta, V.K., Mosquera, E., Gracia, F., Narayanan, V. & Stephen, A. (2015). ZnO/Ag/CdO nanocomposite for visible light-induced photocatalytic degradation of industrial textile effluents, *Journal of Colloid and Interface Science*, 452, pp. 126–133, DOI: 10.1016/j.jcis.2015.04.035.

Seng-eiad, S. & Jitkarnka, S. (2016). Untreated and HNO_3-treated pyrolysis char as catalysts for pyrolysis of waste tire: in-depth analysis of tire-derived products and char characterization, *Journal of Analytical and Applied Pyrolysis*, 122, pp. 151–159, DOI: 10.1016/j.jaap.2016.10.004.

Sharma, V.K., Mincarini, M., Fortuna, F., Cognini, F. & Cornacchia, G. (1998). Disposal of waste tyres for energy recovery and safe environment–review, *Energy Conversion and Management*, 39, 5–6, pp. 511–528, DOI: 10.1016/S0196-8904(97)00044-7.

Sienkiewicz, M., Kucinska-Lipka, J., Janik, H. & Balas, A. (2012). Progress in used tyres management in the European Union: a review, *Waste Management*, 32, 10, pp. 1742–1751, DOI: 10.1016/j.wasman.2012.05.010.

Tan, I.A.W., Ahmad, A.L. & Hameed, B.H. (2008). Preparation of activated carbon from coconut husk: optimization study on removal of 2,4,6-trichlorophenol using response surface methodology, *Journal of Hazardous Materials*, 153, 1–2, pp. 709–717, DOI: 10.1016/j.jhazmat.2007.09.014.

Uzun, Y. & Sahan, T. (2017). Optimization with response surface methodology of biosorption conditions of Hg(II) ions from aqueous media by Polyporus squamosus fungi as a new biosorbent, *Archives of Environmental Protection*, 43, 2, pp. 37–43, DOI: 10.1515/aep-2017-0015.

Zulkali, M.M.D., Ahmad, A.L. & Norulakmal, N.H. (2006). Oryza sativa L. husk as heavy metal adsorbent: optimization with lead as model solution, *Bioresource Technology*, 97, 1, pp. 21–25, DOI: 10.1016/j.biortech.2005.02.007.